

# Thermal Conductivity of Liquid Poly(organosiloxane)s

Vladilen G. Nemzer,\* Boris V. Nemzer, and Leonid V. Nemzer

Oil Institute, Thermophysics Research Center, Scientific Research Institute, Chemical Research Laboratory, Grozny, Russia

This paper describes an apparatus for the measurement of thermal conductivity and reports the thermal conductivity of poly(organosiloxane) liquids. Experimental results are presented for the thermal conductivity of nineteen poly(organosiloxane) liquids (molecular mass from 272 to 14 887 g/mol) of three homologous series (five poly(ethylsiloxane)s, ten poly(methylsiloxane)s, and four poly(phenylmethylsiloxane)s) at atmospheric pressure in the temperature range of 293 K to 623 K. The maximum relative measurement error is  $\pm 1.5\%$ .

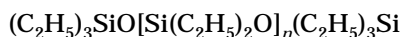
## Introduction

Poly(organosiloxane) (POS) liquids are used in various branches of industry as dielectrics, heat carriers, lubricants, and oils. They are used for hydraulic, damping, and apparatus installations and for vacuum and diffusion pumps.

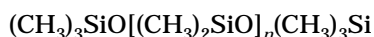
The poly(organosiloxane) liquids are polymers with a linear structure. The molecules of POS consist of large quantities of interchanging silicon and oxygen atoms, and free valences of silicon are replaced by ethyl, methyl, or phenylmethyl radicals.

The formulas for these liquids have the following forms:

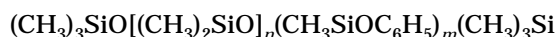
poly(ethylsiloxane)



poly(methylsiloxane)



poly(phenylmethylsiloxane)



where  $n$  and  $m$  are the degrees of polymerization.

POS are transparent liquids, have no odor, and are soluble in aromatic hydrocarbons and ethers but are not soluble in water. Their characteristics make them highly compatible with mineral oils.

## Experimental Section

The research on the thermal conductivity of poly(organosiloxane) liquids in the temperature range of 293 K to 623 K was conducted using a measuring unit consisting of coaxial cylinders with spherical surfaces at the end faces, which is shown in Figure 1. The inner cylinder of the measuring unit has a diameter of  $(34.43 \pm 0.001)$  mm and a cylindrical length of  $(99.8 \pm 0.005)$  mm. On the axis of the cylinder an aperture with a diameter of 3.8 mm was drilled, and an electrical heater was installed in it. The heater was made from constantan wire with a diameter of 0.18 mm wound on a thin porcelain tube and was isolated from the cylinder by a glass fiber. Copper wires of diameter 0.25 mm were welded to the ends of the heater. The outside cylinder has a length of  $(364 \pm 0.005)$  mm and an outside diameter of  $(72 \pm 0.001)$  mm, and the inner diameter of the working part is  $(36.53 \pm 0.001)$  mm. From above and from below, end pieces with half-spherical

surfaces were inserted in the outside cylinder. These made a slide fit to the outside cylinder, and they were connected to it by special flanges.

The inner cylinder was centered in the outside cylinder through seven porcelain struts with a diameter of 1 mm. The cylinders were made of copper, and their working surfaces were carefully ground, then chrome plated, and polished. The spacing between the cylinders was checked using a set of calibrated round feelers. Measurements have shown that the eccentricity does not exceed 0.01 mm.

To install the thermocouples in the outer and inner cylinders, three pairs of contiguous apertures of diameter 2 mm were drilled  $120^\circ$  apart, one member of the pair in each cylinder.

The distance of these thermocouples from the working surfaces of the cylinder was 0.5–1 mm.

The thermocouple wires of three thermocouples and the wires of an electrical heater were introduced from the inner cylinder on a fluoroplastic tube. The tube making contact with the inner cylinder was sealed to the end piece with a special nut and gasket.

The measuring unit was located in a thermostating enclosure of length 500 mm. The enclosure was made from a stainless steel tube pressed onto massive copper cylinders, on the surface of which was a spiral channel of rectangular cross section. Through this channel thermostating liquid could be pumped. The thermostating enclosure also has electrical heating, which was used at temperatures above 483 K. On the thermostating enclosure there were three heaters—the main heater and two security heaters. The capacity of the main heater was 1.5 kW and of the security heater was 0.35 kW. By thermostating the measuring unit using the electrical heaters steady state temperatures were reached 3.5 to 4 h after the beginning of the experiment.

For the creation of a more uniform temperature in the measuring unit, the end faces of the thermostating enclosure were closed by massive end corks, which were well heated by security heaters. For reduction of the heat losses, the thermostating enclosure was isolated from the environment by a thick layer of asbestos.

The temperature gradient in the measuring unit was controlled by two differential thermocouples. At 613 K the temperature difference between the middle and end faces of the measuring unit was not more than 0.02 K.

The measuring unit was filled using a syringe attached to a thin-walled capillary of stainless steel. For a more complete removal of air dissolved in the liquids and

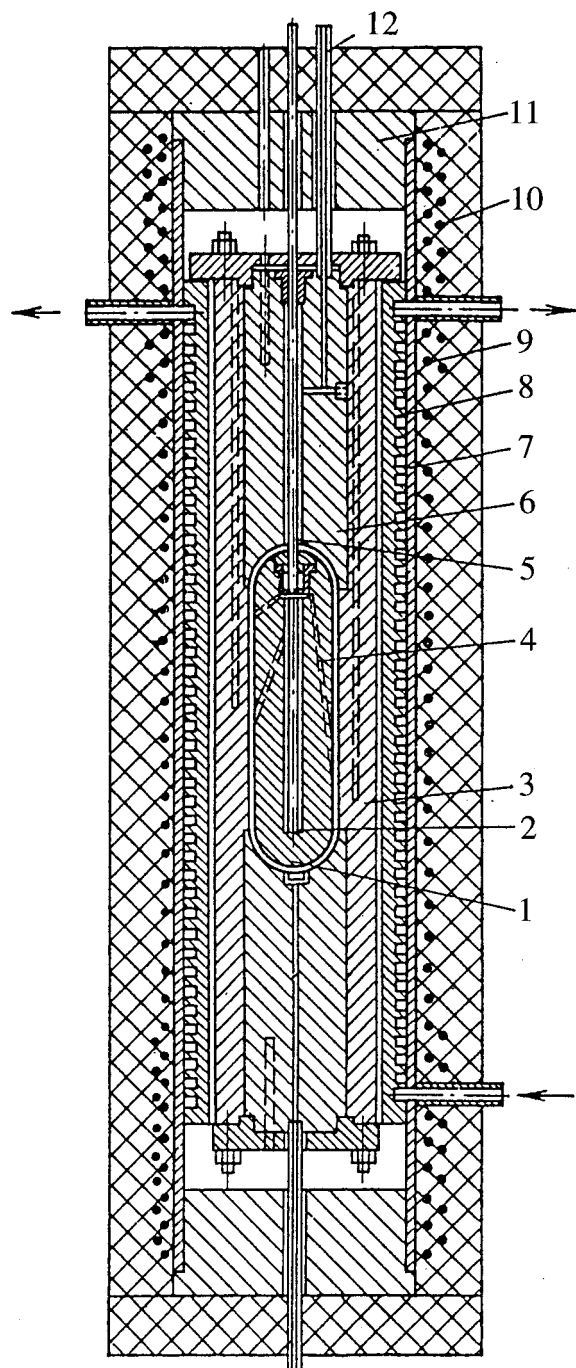


**Figure 1.** General view of the measuring unit and thermostating enclosure: (1) inner cylinder; (2) electric heater; (3) outside cylinder; (4) apertures of thermocouples; (5) fluoroplastic tube; (6) upper inset; (7) stainless steel tube; (8) copper cylinder; (9) main heater; (10) security heaters; (11) massive cork; (12) metal capillaries.

absorbed on the working surfaces, the measuring unit and liquid were heated up (about to the normal boiling temperature) and then the liquid was repeatedly passed through the measuring unit using the syringe.

A battery of accumulators served as the source of the power supply for the heater of the measuring unit inner cylinder. The current in the heater circuit was determined from the voltage across the standard resistor of class  $\pm 0.01\%$ . The voltage across the standard resistor and the electric heater were measured by potentiometers.

The temperature difference in the layer of the liquid was measured using three nichrome-constantan thermocouples. The emf of the thermocouples was measured by

a potentiometer. The error in the measurement of a temperature difference is estimated to be  $\pm 0.005$  K. To avoid the effects of parasitic emf's, all measurements were made in two directions of current. The thermal conductivity at each temperature was measured for various differences of temperature in the layer and  $Gr \cdot Pr < 1000$ , where  $Gr$  and  $Pr$  are the Grashof and Prandtl criterion parameters.

The maximum relative error of measurement of thermal conductivity using the described installation was  $\pm 1.5\%$ .

The thermal conductivity of the liquids was calculated using the equation

$$IU - \sum Q_0 = \frac{2\pi\lambda\Delta t_m h}{\ln \frac{D}{d}} + 2\frac{\pi\lambda\Delta t_m Dd}{D-d}$$

where

$$\lambda = \frac{IU - \sum Q_0}{2\pi\Delta t_m \left( \frac{h}{\ln \frac{D}{d}} + \frac{Dd}{D-d} \right)} = \frac{IU - \sum Q_0}{A\Delta t_m} \quad (1)$$

where  $A$  is the geometric constant of the measuring unit,  $I$  is the current in the heater circuit,  $U$  is the correction to the voltage on the copper current lead wires,  $\sum Q_0$  is the correction on the loss of heat from the inner cylinder,  $h$  is the length of the cylinders part inner cylinder,  $D$  and  $d$  are the diameters of the working part of the outside and inside cylinders,  $\Delta t_m$  is the measured temperature difference in the layer.

In the calculation of the thermal conductivity, the corrections due to mispositioning of thermocouples, temperature change of the geometrical sizes of the measuring unit, and outflow of heat on the struts, fluoroplastic tube, and wires were accounted for.

In light of the large thermal conductivity of copper, the correction on the thermocouple set in the experiment did not exceed 0.1–0.2% for  $t_m$ .

The value of  $A$  depends on the geometrical sizes of the measuring unit and is temperature dependent.

$$A_T = A_{293} + K(T - 293) \quad (2)$$

where  $A_{293} = 14.34$  m and  $K = 0.005$  m·K<sup>-1</sup>.

Correction for this effect at a temperature of 613 K amounts to 1.12%. The size of the correction due to the loss of heat energy in the centering struts was not more than 0.03–0.04%.

For the calculation of correction for heat losses on the fluoroplastic tube and wires, the tube and wires were provisionally replaced by a rod with an equivalent thermal conductivity, but with the same sizes. We considered that the spacing between the rod and outside cylinder was filled by a liquid under investigation, and the temperature of the outside cylinder along the rod was constant and equal to  $T_2$ . The temperature at the beginning of a rod was equal to the temperature of the cylinder  $T_1$ , and that at the end of rod was  $T_2$  (Figure 2). Special measurements have confirmed the equality of temperatures of the end of a rod and the outside cylinder.

The equation for the thermal balance for an element of the length of a rod is

$$Q_1 - Q_2 = dQ = \lambda_{eq} \frac{\partial^2 \vartheta}{\partial x^2} dx \quad (3)$$

where  $dQ$  can also be written as

$$dQ = \frac{2\pi\lambda\vartheta dx}{\ln \frac{d_1}{d_0}} \quad (4)$$

where  $\lambda_{\text{eq}}$  is the equivalent thermal conductivity of the rod and  $f$  is the cross sectional area of the rod.

When we set eq 3 equal to eq 4, we get

$$\frac{\partial^2 \vartheta}{\partial x^2} - m^2 \vartheta = 0 \quad (5)$$

where

$$m = \pm \sqrt{\frac{2\pi\lambda}{\lambda_{\text{eq}} f \ln \frac{d_1}{d_0}}} \quad (6)$$

The integral of the differential (5) takes the following form:

$$\vartheta = C_1 \exp(mx) + C_2 \exp(-mx) \quad (7)$$

For a rod of a finite length:

$$\text{at } x = 0 \quad \vartheta = \vartheta_0, \vartheta_0 = C_1 + C_2$$

at  $x = L$

$$\vartheta = 0, (\partial\vartheta/\partial x)_{x=L} = C_1 m \exp(mL) - C_2 m \exp(-mL) \quad (8)$$

The amount of energy dissipated by the rod can be determined as

$$Q_0 = -\lambda_{\text{eq}} f (\partial\vartheta/\partial x)_{x=0} = -\lambda_{\text{eq}} f m (C_1 - C_2) \quad (9)$$

From eq 8 we find  $C_1$  and  $C_2$ .

Substituting these into eq 9, we get the equation in its final form:

$$Q_0 = m \lambda_{\text{eq}} f \vartheta_0 \text{th}(mL) \quad (10)$$

where  $\text{th}(mL)$  is a hyperbolic tangent. In our case  $L/d_0 = 32$  and  $\text{th}(mL) = 1$ .

Our calculations have shown that the correction on outflow of energy on the fluoroplastic tube and wires does not exceed 0.7%.

For improvement of this technique on the installation described above, the thermal conductivities of distilled water, toluene, and benzene up to the normal boiling temperature, and also air up to 573 K, were measured. In calculation of the thermal conductivity of air, besides the corrections mentioned above, we included the correction for radiation, which at the temperature of 573 K,  $\Delta t_m = 5$  K, and degree of blackness of the radiating surface equaling  $\epsilon_1 = \epsilon_2 = 0.06$ , constituted 3.3%. The total correction constituted 5.7%.

The thermal conductivity of all investigated liquids and air with error up to 1.1% can be described by a linear equation. Table 1 gives the measured thermal conductivity  $\lambda_0$  of the reference fluid at 303 K and the measured temperature coefficient  $\alpha$  along with additional properties.

Our experimental data on the thermal conductivity for toluene, benzene, water, and air over our research range of temperature are well consistent with the data of other scientists (Vargaftic, 1949; Filippov, 1953; Riedel, 1951; Schmidt and Leidenfrost, 1954; Ziebland and Burton, 1961; Rastorguev and Geller, 1967; Filippov, 1954; Vargaftic, 1963). The difference is no more than  $\pm 1.5\%$ .

In calculating the thermal conductivity of a liquid, the correction for radiation is not usually taken into account,

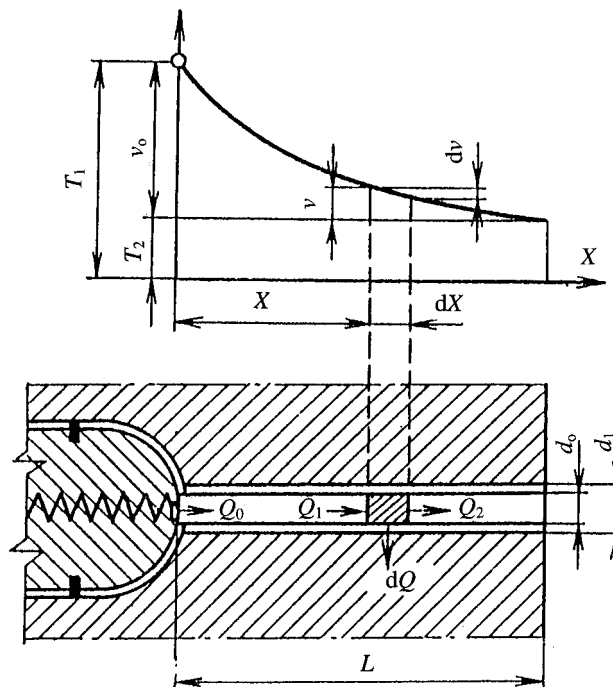


Figure 2. Scheme of the calculation of heat outflow on the fluoroplastic tube and wires.

Table 1. Thermal Conductivity of the Investigated Liquids and Air

| product | $\rho_0/\text{kg}\cdot\text{m}^{-3}$ | $n_0^r$ | $\lambda_0/\text{W}\cdot\text{m}^{-1}\cdot\text{K}^{-1}$ | $10^2\alpha/\text{K}^{-1}$ |
|---------|--------------------------------------|---------|--|----------------------------|
| toluene | 866.5                                | 1.4965  | 0.1340   | -0.187                     |
| phenol  | 878.2                                | 1.5011  | 0.1430   | -0.154                     |
| water   |                                      |         | 0.6230   | +0.176                     |
| air     |                                      |         | 0.0264   | +0.260                     |

because it is considered insignificant. However, Dick and McCready (1954), while measuring the thermal conductivity of an organic liquid by the slab method, noticed that with an increase in the thickness of the liquid layer from 0.6 to 2.2 mm its thermal conductivity increases (approximately by 7.8% at the temperature of 333 K).

The increase in thermal conductivity with the increase in thickness of the liquid may be caused by heat transfer by radiation through the layer of liquid under examination.

$$\lambda_{\text{ef}} = \lambda + \lambda_r \quad (11)$$

where  $\lambda_{\text{ef}}$  is the measurement of the effectiveness value of thermal conductivity,  $\lambda$  is the molecular thermal conductivity, and  $\lambda_r$  is the radiation thermal conductivity.

In Poltz's work, the influence of heat radiation on heat transfer in liquids is considered (Poltz, 1965a,b; Fritz and Poltz, 1962; Poltz and Jugel, 1967). He believes, and confirms this with experiments, that the fraction of radiation in liquids with relatively small optical density in the infrared range may reach high values, especially at high temperatures.

While considering the problem of joint heat transfer with thermal conductivity and radiation through a layer of absorbent medium situated between two infinitely large parallel plates, Poltz (1965) derived

$$q_\Lambda = \frac{16}{3} \frac{n^2 \sigma_0 T^3}{\bar{a}} Y \frac{\Delta t_m}{\delta} = \lambda_r \frac{\Delta t_m}{\delta} \quad (12)$$

where  $n$  is the coefficient refraction of the medium;  $\sigma_0$  is the Stefan-Boltzmann constant,  $\sigma_0 = 5.67 \times 10^{-8} \text{ W/m}^2\cdot\text{K}$ ;  $\bar{a}$  is the average integral value of the fluid absorptancy coefficient,  $\text{m}^{-1}$ ;  $\delta$  is the thickness of layer,  $\text{m}$ ;  $\tau = \bar{a}\delta$  is

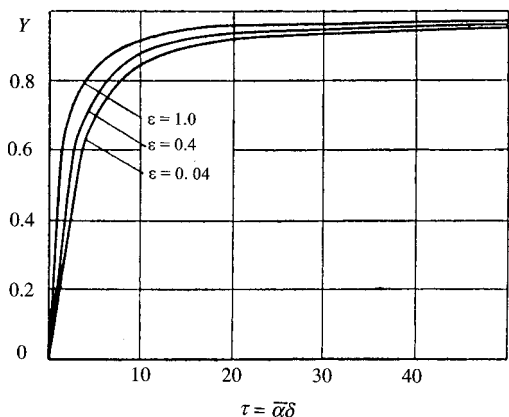


Figure 3. Dependence of  $\tau = f(\epsilon, Y)$ .

the optical density of the medium;  $T$  is temperature of the medium, K; and  $\lambda_r$  is the proportion coefficient (radiation thermal conductivity coefficient).

The value of  $Y = f(\epsilon, \tau)$  is tabulated by Poltz (1965), and the graph can be found in Figure 3.

For the marginal condition, the function  $Y$  takes on the following values:

$$\text{at } \tau \rightarrow 0 \quad Y_{\tau \rightarrow 0} = \frac{3}{4} \frac{\epsilon}{2 - \epsilon}$$

$$\text{at } \tau \rightarrow \infty \quad Y_{\tau \rightarrow \infty} = 1$$

For calculating  $\lambda_r$ , it is necessary to know the degree of blackness,  $\epsilon$ , of the radiating surface and optical density,  $\tau = \bar{a}\delta$ , of the fluid in question. However, the existing literature almost never mentions any results pertaining to the spectral dependence of absorbance of organic liquids for radiation in the whole infrared range. This makes correct estimation of the value of  $\bar{a}$  for a number of liquids practically impossible. Assuming (Poltz, 1965) for toluene, for the wavelengths in the interval from  $2\mu$  to  $15\mu$ ,  $\bar{a} = 3.5 \text{ m}^{-1}$ , the correction for radiation at 298 K is 2.3% and at 373 K is 5.2% ( $n = 1.5$ ), according to Dick and McCreedy (1954).

Accounting for this correction, in the temperature range under consideration, our data for toluene are higher than Poltz's by 2.5% at zero slit width. Taking into consideration the dependence of  $n$  on temperature, the correction for radiation is 4.2%.

For the wavelengths in the interval from  $6.5$  to  $15.5\mu$ , using the absorbancy spectrum of toluene, we get  $\bar{a} = 11 \text{ m}^{-1}$ . In this case, the correction for radiation ( $n = 1.5$ ) at 293 K is 1.06% and at 373 K is 2.4%.

For a more accurate estimate of the influence of radiation on the heat transfer in fluids, and to verify the correctness of the equation, it was necessary to conduct experiments to measure the thermal conductivity of liquids in layers of different geometrical shapes and sizes and at different degrees of blackness of the radiating surfaces. It was also necessary to have reliable data on absorbancy spectra of liquids in the infrared radiation region at different temperatures.

For development of correction methods, experiments were conducted to determine critical values of the Gr·Pr. The dependence of  $\epsilon = \lambda_{\text{eq}}/\lambda$  on Gr·Pr is depicted in Figure 4. From Figure 4, it is clear that convection in a cylindrical layer with a slit of 1.05 mm, with ratio  $D/d = 1.06$ , takes place at  $\text{Gr} \cdot \text{Pr} \geq 1700$ .

The thermal conductivity in this work was measured at different  $\Delta t_m$  in the layer (1.8–3 K) and  $\text{Gr} \cdot \text{Pr} < 1000$ ; so there was an absence of convection.

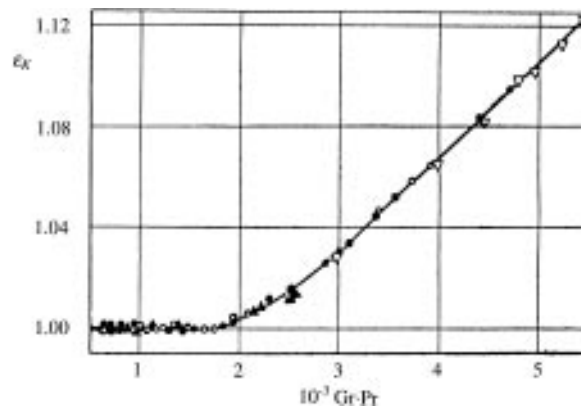


Figure 4. Dependence of the convection coefficient  $\epsilon_k$  on Gr·Pr: (●) toluene; (▲) benzene; (◻) acetone; (▽) *n*-heptane.

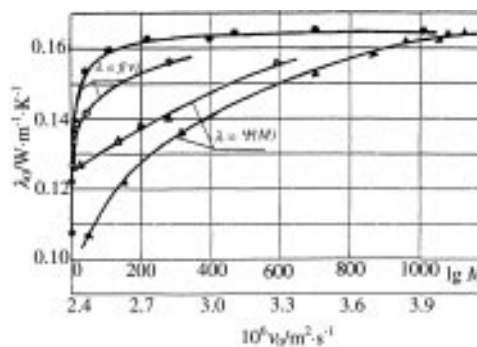


Figure 5. Dependence of the thermal conductivity  $\lambda_0$  on viscosity  $\nu_0$  and molecular mass  $M$ : (●, ▲) PMS; (◻, ◻) PES.

## Results

Using the setup described above, the thermal conductivities of the poly(organosiloxane) liquids were measured at temperatures from 293 K to 623 K.

In Table 2 the following are listed: density at 293 K,  $\rho_0$ ; temperature coefficient of density,  $\beta$ ; viscosity at 293 K,  $\nu_0$ ; refractive index at 293 K,  $n_0^D$ ; molecular mass,  $M$ ; the mean degree of polymerization,  $n$ ; the number of atoms of silicon in molecules, Si; thermal conductivity at 303 K,  $\lambda_0$ ; and temperature coefficient of thermal conductivity,  $\alpha$ .

Molecular masses of poly(organosiloxane) liquids were determined by cryoscopy using benzene and naphthalene as solvents.

The refractive index  $n^D$  was determined by a refractometer.

The density at the temperature of 293 K was determined by a density bottle at constant volume. In the temperature range (293–473) K the density was measured using a special installation using the method of the hydrostatic balance. The maximum relative error was  $\pm 0.07\%$ .

The viscosity was determined on the capillary viscosimeter of the Penkevich type using PMS-100 as a thermostatic liquid. The maximum relative error was no more than  $\pm 2.4\%$  for all liquids.

Experimental data for thermal conductivity are given in Table 3. These data can be described by a linear equation with an error of 0.8%.

$$\lambda_r = \lambda_0 [1 + \alpha(T/K - 303)] \quad (13)$$

The deviation of the values calculated with (13) from the experimental data does not exceed the error of experiment.

Polytherms of the thermal conductivity for substances in the same series lie higher with increasing molecular mass.

**Table 2. Characteristics of the Poly(organosiloxane) Liquids**

| polymer   | $\rho_0/\text{kg m}^{-3}$ | $10^2\beta/\text{K}^{-1}$ | $n_0^r$ | $10^6\nu_0/\text{m}^2\cdot\text{s}^{-1}$ | $M/\text{g mol}^{-1}$ | $n$ | Si  | $\lambda_0/W\cdot\text{m}^{-1}\text{K}^{-1}$ | $10^2\alpha/\text{K}^{-1}$ |
|-----------|---------------------------|---------------------------|---------|--|-----------------------|-----|-----|--|----------------------------|
| PMS-1.5   | 850.11                    | 0.116                     | 1.3893  | 1.52                                     | 298                   | 2   | 4   | 0.107  | 0.126                      |
| PMS-5     | 911.73                    | 0.099                     | 1.3987  | 5.17                                     | 431                   | 4   | 6   | 0.121  | 0.120                      |
| PMS-10    | 937.65                    | 0.093                     | 1.4018  | 9.84                                     | 739                   | 8   | 10  | 0.136  | 0.118                      |
| PMS-50    | 959.21                    | 0.088                     | 1.4047  | 42.45                                    | 2975                  | 38  | 40  | 0.153  | 0.113                      |
| PMS-100   | 968.45                    | 0.087                     | 1.4047  | 107.98                                   | 5011                  | 66  | 68  | 0.159  | 0.110                      |
| PMS-200   | 970.12                    | 0.087                     | 1.4054  | 216.42                                   | 6675                  | 88  | 90  | 0.162  | 0.111                      |
| PMS-400   | 971.81                    | 0.086                     | 1.4059  | 395.51                                   | 9634                  | 128 | 130 | 0.163  | 0.106                      |
| PMS-476   | 972.45                    | 0.086                     | 1.4061  | 467.14                                   | 10189                 | 136 | 138 | 0.164  | 0.110                      |
| PMS-700   | 972.98                    | 0.085                     | 1.4049  | 698.17                                   | 12336                 | 164 | 166 | 0.165  | 0.107                      |
| PMS-1000  | 973.06                    | 0.085                     | 1.4058  | 1013.85                                  | 14887                 | 198 | 200 | 0.165  | 0.105                      |
| PES-1     | 869.94                    | 0.090                     | 1.4361  | 3.18                                     | 272                   | 1   | 3   | 0.128  | 0.131                      |
| PES-2     | 913.40                    | 0.089                     | 1.4398  | 10.80                                    | 392                   | 2   | 4   | 0.133  | 0.121                      |
| PES-3     | 947.41                    | 0.080                     | 1.4392  | 13.96                                    | 495                   | 3   | 5   | 0.137  | 0.115                      |
| PES-4     | 957.80                    | 0.076                     | 1.4425  | 51.52                                    | 626                   | 4   | 6   | 0.141  | 0.101                      |
| PES-5     | 991.00                    | 0.070                     | 1.4468  | 268.80                                   | 1607                  | 14  | 16  | 0.156  | 0.088                      |
| PFMS-2/5L | 1019.64                   | 0.077                     | 1.4993  | 17.04                                    | 570                   | 3   | 5   | 0.128  | 0.105                      |
| PFMS-4    | 1102.30                   | 0.065                     | 1.5329  | 658.82                                   | 1328                  | 9   | 11  | 0.148  | 0.084                      |
| FM-1322   | 999.87                    | 0.062                     | 1.4517  | 23.48                                    | 1083                  | 10  | 12  | 0.142  | 0.107                      |
| PFMS-6    | 1150.14                   |                           | 1.5837  |  | 1664                  | 10  | 12  | 0.150  | 0.100                      |

**Table 3. Thermal Conductivity of the Poly(organosiloxane) Liquids**

| polymer   | $T/\text{K}$                               |        |        |        |        |        |        |        |        |        |
|-----------|--|--------|--------|--------|--------|--------|--------|--------|--------|--------|
|           | 293  | 313    | 333    | 353    | 373    | 393    | 413    | 433    | 453    | 473    |
|           | $\lambda/W\cdot\text{m}^{-1}\text{K}^{-1}$ |        |        |        |        |        |        |        |        |        |
| PMS-1.5   | 0.1082                                     | 0.1061 | 0.1034 | 0.1003 | 0.0976 | 0.0949 | 0.0922 | 0.0865 | 0.0868 | 0.0841 |
| PMS-5     | 0.1221                                     | 0.1204 | 0.1173 | 0.1142 | 0.1112 | 0.1085 | 0.1053 | 0.1021 | 0.0992 | 0.0963 |
| PMS-10    | 0.1384                                     | 0.1342 | 0.1311 | 0.1283 | 0.1255 | 0.1220 | 0.1182 | 0.1153 | 0.1121 | 0.1093 |
| PMS-50    | 0.1553                                     | 0.1514 | 0.1483 | 0.1441 | 0.1412 | 0.1375 | 0.1343 | 0.1313 | 0.1270 | 0.1241 |
| PMS-100   | 0.1614                                     | 0.1572 | 0.1543 | 0.1501 | 0.1474 | 0.1432 | 0.1405 | 0.1362 | 0.1333 | 0.1292 |
| PMS-200   | 0.1643                                     | 0.1604 | 0.1572 | 0.1532 | 0.1492 | 0.1461 | 0.1423 | 0.1393 | 0.1354 | 0.1314 |
| PMS-400   | 0.1651                                     | 0.1612 | 0.1580 | 0.1542 | 0.1513 | 0.1471 | 0.1442 | 0.1412 | 0.1372 | 0.1341 |
| PMS-476   | 0.1662                                     | 0.1624 | 0.1593 | 0.1554 | 0.1514 | 0.1482 | 0.1443 | 0.1411 | 0.1371 | 0.1347 |
| PMS-700   | 0.1673                                     | 0.1633 | 0.1604 | 0.1561 | 0.1532 | 0.1490 | 0.1462 | 0.1424 | 0.1393 | 0.1354 |
| PMS-1000  | 0.1672                                     | 0.1631 | 0.1603 | 0.1560 | 0.1534 | 0.1491 | 0.1461 | 0.1433 | 0.1392 | 0.1365 |
| PES-1     | 0.1301                                     | 0.1262 | 0.1232 | 0.1202 | 0.1163 | 0.1135 | 0.1104 | 0.1061 | 0.1034 | 0.0995 |
| PES-2     | 0.1350                                     | 0.1314 | 0.1284 | 0.1254 | 0.1221 | 0.1191 | 0.1155 | 0.1120 | 0.1091 | 0.1064 |
| PES-3     | 0.1392                                     | 0.1353 | 0.1323 | 0.1291 | 0.1264 | 0.1233 | 0.1203 | 0.1172 | 0.1133 | 0.1101 |
| PES-4     | 0.1421                                     | 0.1401 | 0.1374 | 0.1343 | 0.1310 | 0.1281 | 0.1252 | 0.1234 | 0.1202 | 0.1172 |
| PES-5     | 0.1573                                     | 0.1553 | 0.1523 | 0.1492 | 0.1463 | 0.1440 | 0.1413 | 0.1382 | 0.1354 | 0.1330 |
| PFMS-2/5L | 0.1294                                     | 0.1272 | 0.1251 | 0.1230 | 0.1202 | 0.1174 | 0.1142 | 0.1110 | 0.1093 | 0.1071 |
| PFMS-4    | 0.1492                                     | 0.1460 | 0.1433 | 0.1411 | 0.1383 | 0.1362 | 0.1330 | 0.1313 | 0.1292 | 0.1263 |
| FM-1322   | 0.1430                                     | 0.1400 | 0.1371 | 0.1334 | 0.1303 | 0.1272 | 0.1241 | 0.1225 | 0.1182 | 0.1151 |
| PFMS-6    | 0.1524                                     | 0.1482 | 0.1454 | 0.1423 | 0.1391 | 0.1363 | 0.1330 | 0.1304 | 0.1282 | 0.1251 |
|           | $T/\text{K}$                               |        |        |        |        |        |        |        |        |        |
|           | 493  | 513    | 533    | 553    | 573    | 593    | 613    | 633    | 653    |        |
|           | $\lambda/W\cdot\text{m}^{-1}\text{K}^{-1}$ |        |        |        |        |        |        |        |        |        |
| PMS-1.5   | 0.0814                                     | 0.0787 | 0.0760 | 0.0733 | 0.0706 |        |        |        |        |        |
| PMS-5     | 0.0934                                     | 0.0905 | 0.0876 | 0.0847 | 0.0818 |        |        |        |        |        |
| PMS-10    | 0.1063                                     | 0.1021 | 0.0990 | 0.0959 | 0.0927 | 0.0895 |        |        |        |        |
| PMS-50    | 0.1203                                     | 0.1174 | 0.1132 | 0.1105 | 0.1063 | 0.1034 |        |        |        |        |
| PMS-100   | 0.1266                                     | 0.1222 | 0.1191 | 0.1152 | 0.1123 | 0.1084 |        |        |        |        |
| PMS-200   | 0.1280                                     | 0.1243 | 0.1216 | 0.1172 | 0.1133 | 0.1102 |        |        |        |        |
| PMS-400   | 0.1303                                     | 0.1274 | 0.1231 | 0.1203 | 0.1164 | 0.1131 |        |        |        |        |
| PMS-476   | 0.1304                                     | 0.1263 | 0.1232 | 0.1191 | 0.1153 | 0.1123 |        |        |        |        |
| PMS-700   | 0.1312                                     | 0.1283 | 0.1241 | 0.1214 | 0.1173 | 0.1141 |        |        |        |        |
| PMS-1000  | 0.1323                                     | 0.1294 | 0.1251 | 0.1223 | 0.1182 | 0.1150 |        |        |        |        |
| PES-1     | 0.0961                                     | 0.0928 | 0.0894 |        |        |        |        |        |        |        |
| PES-2     | 0.1022                                     | 0.0992 | 0.0960 |        |        |        |        |        |        |        |
| PES-3     | 0.1070                                     | 0.1044 | 0.1014 |        |        |        |        |        |        |        |
| PES-4     | 0.1143                                     | 0.1112 | 0.1083 |        |        |        |        |        |        |        |
| PES-5     | 0.1303                                     | 0.1274 | 0.1241 | 0.1220 | 0.1193 |        |        |        |        |        |
| PFMS-2/5L | 0.1031                                     | 0.1003 | 0.0975 | 0.0948 | 0.0924 | 0.0893 | 0.0866 | 0.0839 | 0.0811 |        |
| PFMS-4    | 0.1243                                     | 0.1213 | 0.1192 | 0.1161 | 0.1143 | 0.1112 | 0.1094 | 0.1061 | 0.1043 |        |
| FM-1322   | 0.1122                                     | 0.1093 | 0.1064 | 0.1031 | 0.1002 | 0.0973 | 0.0942 | 0.0912 | 0.0882 |        |
| PFMS-6    | 0.1220                                     | 0.1192 | 0.1161 | 0.1133 | 0.1101 | 0.1072 | 0.1042 | 0.1013 | 0.0975 |        |

As Figure 5 shows, the thermal conductivity of PMS increases with increasing molecular mass, faster at first but with a decreasing rate of increase as it tends toward an upper limit.

Polytherms of thermal conductivity for PES lie higher than those for PMS at the same molecular mass. The substitution of methylsiloxy bonds for methylphenylsiloxy

bonds, for example PMS-5 for PFMS-2/5L (they have almost equal molecular masses), increases the thermal conductivity (Table 2). With an increase of the kinematic viscosity, the thermal conductivity increases strongly at first, then more slowly, tending toward a limit.

Figure 6 shows the relation  $\lambda_T = f(\rho_T)$  for PMS. Each solid line is for a different PMS molecular mass. As the

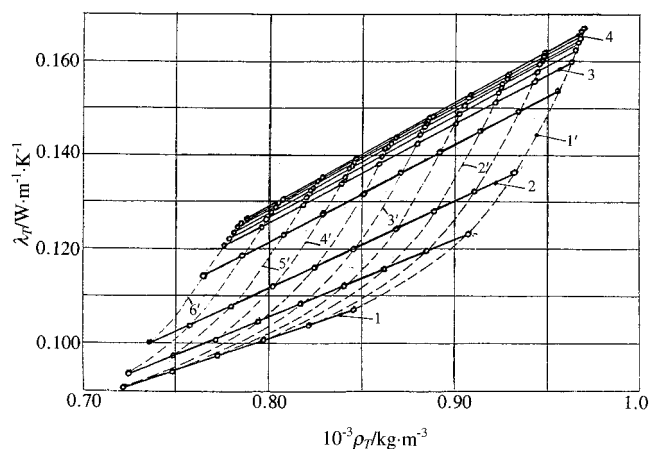


**Figure 6.** Dependence of the thermal conductivity  $\lambda_T$  on density  $\rho_T$  for PMS [(1) PMS-1.5; (2) PMG-10; (3) PMS-100; (4) PMS-1000] and for isotherm [(1') 293 K; (2') 348 K; (3') 398 K; (4') 448 K; (5') 473 K; (6') 523 K].

number of Si atoms increases, these lines lie higher on the diagram, and the distance between lines  $\lambda_T = f(\rho_T)$  de-

creases. Figure 6 is of definite practical interest, because it allows us to determine the thermal conductivity when we know the density.

#### Literature Cited

- (1) Dick, M. F.; McCready, D. W. *Trans. ASME* **1954**, *76*, 881.
- (2) Filippov, L. *News MGU* **1953**, *9*, 17.
- (3) Filippov, L. *News MGU* **1954**, *12*, 24.
- (4) Fritz, W.; Poltz, H. *Int. J. Heat Mass Transfer* **1962**, *5*, 307.
- (5) Poltz, H. *Int. J. Heat Mass Transfer* **1965a**, *8*, 609.
- (6) Poltz, H. *Int. J. Heat Mass Transfer* **1965b**, *8*, 515.
- (7) Poltz, H.; Jugel, R. *Int. J. Heat Mass Transfer* **1967**, *10*, 1075.
- (8) Rastorguev, Y.; Geller, V. *I.F.J.* **1967**, *13*, 17.
- (9) Riedel, L. *Chem.-Ing.-Tech.* **1951**, *23*, 321.
- (10) Schmidt, E.; Leidenfrost, W. *Chem.-Ing.-Tech.* **1954**, *1*, 35.
- (11) Vargaftic, N. *News VTI* **1949**, *8*, 36.
- (12) Vargaftic, N. *Directory of thermophysical properties of Gases and Liquids*, 1963.
- (13) Ziebland, H.; Burton, I. *J. Chem. Eng. Data* **1961**, *6*, 27.

Received for review August 26, 1996. Accepted November 21, 1996.®

JE960292C

® Abstract published in *Advance ACS Abstracts*, January 15, 1997.